Supporting materials for

Magnetic topological insulator in two-dimensional $EuCd_2Bi_2$: giant gap with robust topology against magnetic transitions

Hao Wang, Chengwang Niu*, Ning Mao, Xiangting Hu, Baibiao Huang and Ying Dai†

School of Physics, State Key Laboratory of Crystal Materials, Shandong University, Jinan 250100, China

Corresponding authors: c.niu@sdu.edu.cn (C. Niu), daiy60@sdu.edu.cn (Y. Dai)

Computational Methods

The density functional calculations are performed by using the Vienna ab initio simulation package (VASP) and the FLUER code. We use Perdew-Burke-Ernzerhof functional within generalized gradient approximation (GGA) to describe the exchange and correlation interactions of the electrons. In order to simulate a single-layer structure, we use a 20 Å vacuum space in z direction to eliminate the interactions between the periodical imagines. Owing to the Eu atoms contains localized f-state electrons. We consider GGA+U method to correct on-site Coulomb interactions. The value of U_{eff} was set to 7eV for the 4f electrons of Eu atoms. We use a 15×15×1 k-mesh within the Monkhorst-Pack scheme for the self-consistent calculation. In order to calculating the topological properties, we use 3s and 3p orbitals on Cd, 3d and 4f orbitals on Eu, and 5p orbitals on Bi atoms as the projection orbitals to construct the maximally localized Wannier functions as implemented in Wannier90 code.

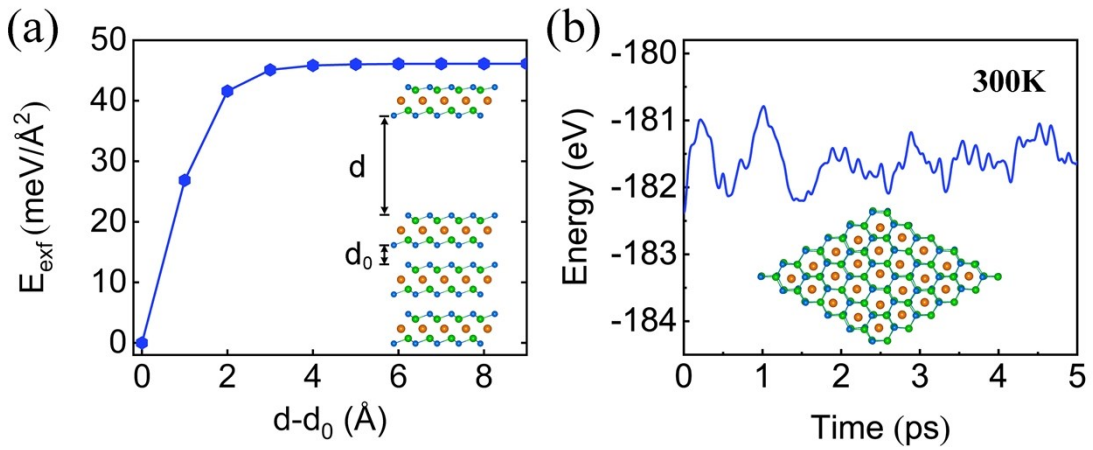

Figure S1. (a) Exfoliation energy of $EuCd_2Bi_2$ QLs. The inset shows the side view of bulk $EuCd_2Bi_2$ and the interlayer distance. (b) Variations of the energy versus the AIMD simulations time for $EuCd_2Bi_2$. The insets denote the top view of 5×5×1 supercell of $EuCd_2Bi_2$ after AIMD simulations lasting for 5 ps at T = 300 K. There is no obvious structural deformation and broken bonds after simulation, which suggests the thermal stability of $EuCd_2Bi_2$ QLs.

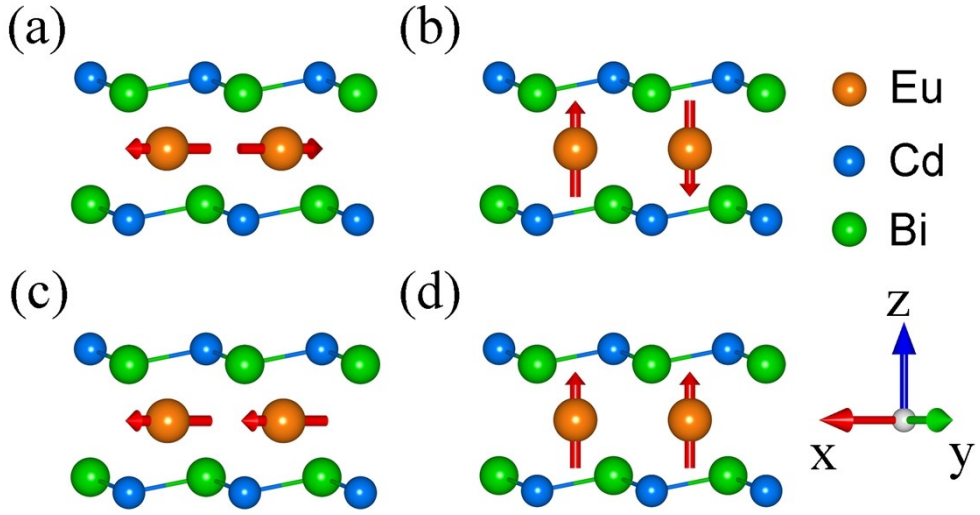

Figure S2. The scheme of the magnetic configurations, where (a)-(d) for in-plane AFM, out-of-plane AFM, in-plane FM, and out-of-plane FM, respectively. The red arrows stand for the direction of the spin moments. The orange, blue and green balls respect for the Eu, Cd and Bi atoms, respectively.

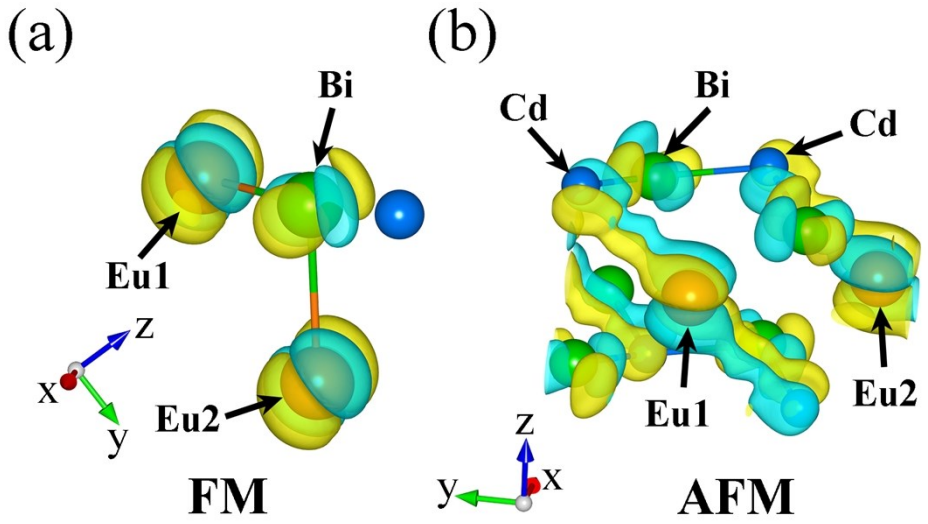

Figure S3. The spin density distribution for (a) the FM state and (b) the AFM state, the yellow and blue area respect for the density of majority spin and minority spin, respectively. The bond angle of Eu1-Bi-Eu2 is 88.8°, (a) shows the Goodenough - Kanamori rules induced FM state, while (b) reveals the super-exchange interactions path of Eu1-Cd-Bi-Cd-Eu2.

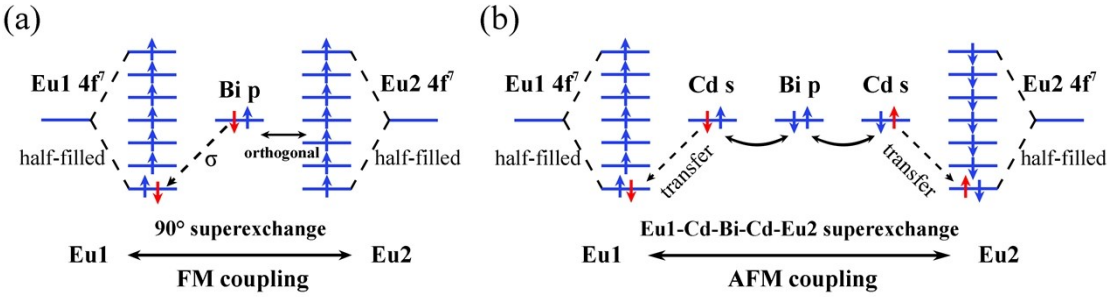

Figure S4. The scheme of super-exchange interactions of different magnetic configurations. The Eu-Bi units construct an octahedron structure, Eu atoms located at the center and Bi atoms act as the ligands, and we simply assume that the energy degeneracy of the f electrons in this octahedral crystal field are completely lifted owing to the perturbation of the Cd atoms. The Eu-Bi-Eu bond angle is 88.8°, approaching the ideal 90°. As the spin density shown in Figure S3(a), the p orbitals of Bi are parallel and perpendicular to Eu1 and Eu2 atom, respectively. So the interaction mechanism of the FM states can be understood by Goodenough - Kanamori rules. However, the AFM state exhibits distinct super-exchange interactions mechanism, as the spin density shown in Figure S3(b), the f orbitals of Eu atom hybrid with the extended s orbital of the nearest-neighbor Cd atom. When the delocalized s electrons of Cd transfer to the f orbital of Eu atom, owing the 4f orbital is half-filled, the spin moments of the remained s electrons of Cd atoms are parallel to the nearest-neighbor Eu atom. In addition, the spin moment is anti-parallel between the Cd and Bi atoms to satisfy the Pauli exclusion principle. The path of the super-exchange interactions is Eu1-Cd-Bi-Cd-Eu2, thus give rising to the AFM coupling. Another evidence about the role of s electrons in the super-exchange interactions can be found in the resolved band structure as shown in the figure 3 of the main text. From figure3 we can derive that, in the AFM state, the s orbital of Cd contributed at Γ point of CBM are higher than that of the FM state, which is attribute to the slightly hybridization between the f electron and s electrons, thus the latter are pushed to a higher energy level.

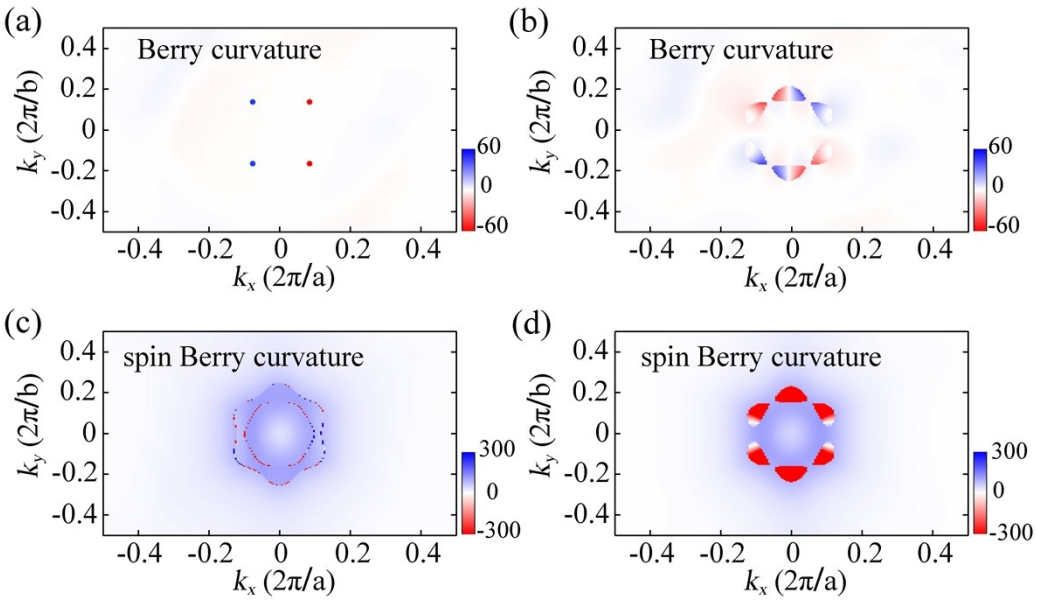

Figure S5. The contour colormap of Berry curvature of (a) in-plane AFM and (b) in-plane FM, respectively (the red and blue dots in (a) are artificially marked for clarify). The contour colormap of spin Berry curvature of (c) in-plane AFM and (d) in-plane FM configurations, respectively. As shown in Figure S5(a), the Berry curvatures of the AFM state have two negative peaks and two positive peaks, the magnitude of these peaks are about 10^3 in unit of $Bohr^2$. On the other hand, the FM state show symmetric six lobes shape. The symmetric distributions of Berry curvature for both FM state and AFM state lead to the integral is zero, as well as the Chern number, thus the $EuCd_2Bi_2$ QLs does not belongs to Chern insulators regardless the magnetic orders.

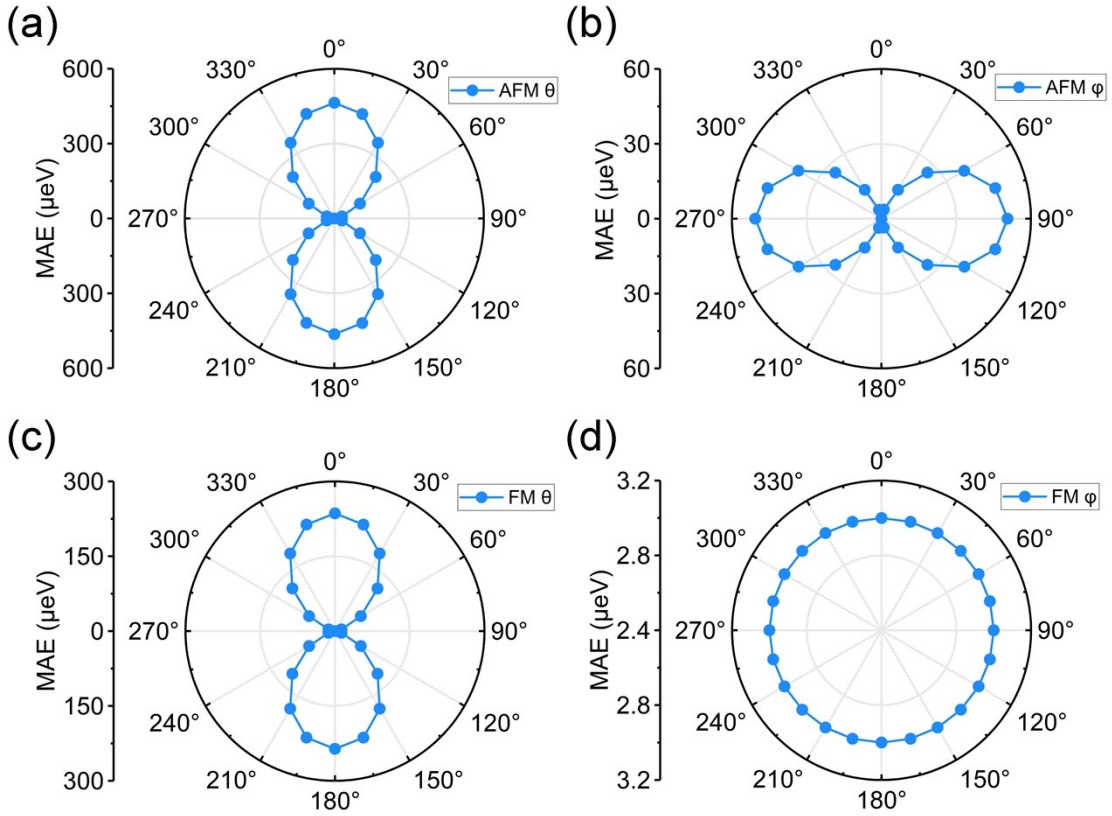

Figure S6. The different angular dependence of magnetic anisotropy energy (MAE) of $EuCd_2Bi_2$: (a) The magnetic moments rotate in xz plane of AFM state. (b) The magnetic moments rotate in xy plane of AFM state. (c) The magnetic moments rotate in xz plane of FM state. (d) The magnetic moments rotate in xy plane of FM state.

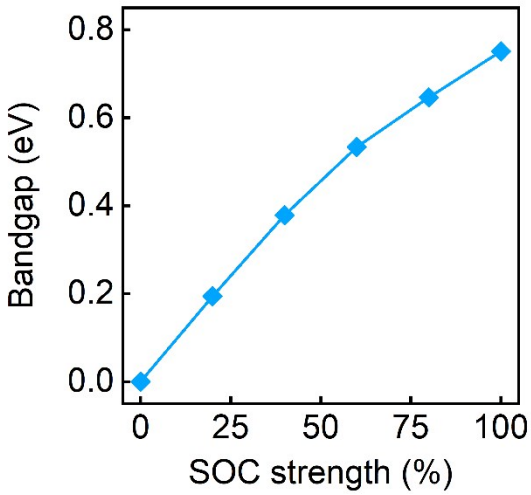

Figure S7. The calculated band gap of 2D AFM $EuCd_2Bi_2$ as a function of SOC strength.

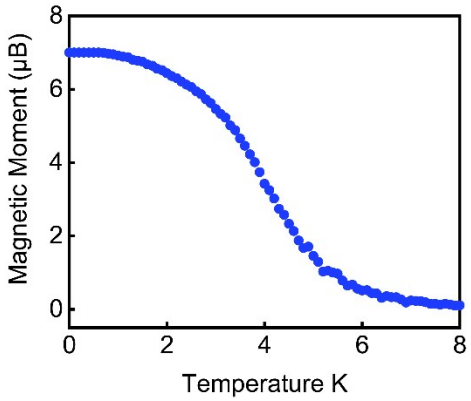

Figure S8. The calculated magnetic moments as a function of temperature for the 2D $EuCd_2Bi_2$.